Hydrodynamic Solutions for a Sonoluminescing Gas Bubble

Ho-Young Kwak and Jung Hee Na
Mechanical Engineering Department, Chung-Ang University, Seoul 156-756, Korea
(Received 13 June 1996)

Analytic solutions for a sonoluminescing gas bubble have been obtained, which provide density, pressure, and temperature distributions for the gas inside a bubble oscillating under an ultrasonic field. The solutions show that sonoluminescence occurs due to the increase and subsequent decrease in bubble wall acceleration which induces a thermal spike. It also turns out that the number of electrons ionized, the ion species, and the kinetic energy of the electrons affect crucially the spectrum of the light emitted. [S0031-9007(96)01702-4]

PACS numbers: 78.60.Mq, 43.25.+y

Sonoluminescence (SL) has been found to be the light emission associated with the catastrophic bubble collapse of a gas bubble oscillating under an ultrasonic field [1]. However, the exact mechanism of the light emission characterized with picosecond flashes of continuous spectrum [2,3] has not been identified as to whether it is of thermal black body and/or bremsstrahlung radiation origin [4,5].

In this study, the density, pressure, and temperature distributions inside a sonoluminescing gas bubble have been obtained by solving the mass, momentum, and energy equations for the gas analytically. The instantaneous radius of a bubble has been obtained by the equation from Keller and Miksis formulation [6]. This equation, including the effects of liquid compressibility, is as follows:

$$\left(1 - \frac{U_b}{C_B}\right)R_b \frac{dU_b}{dt} + \frac{3}{2}U_b^2\left(1 - \frac{U_b}{3C_B}\right) = \frac{1}{\rho_\infty}\left(1 + \frac{U_b}{C_B} + \frac{R_b}{C_B}\frac{d}{dt}\right) \times \left[P_B - P_S\left(t + \frac{R_b}{C_B}\right) - P_\infty\right], \quad (1)$$

where R_b is the bubble radius, U_b is the bubble wall velocity, C_B is the sound speed in liquid at the bubble wall, and ρ_∞ is the medium density. The liquid pressure on the external side of the bubble wall P_B is related to the pressure inside the bubble wall P_B by $P_B = P_b - 2\sigma/R_b - 4\mu U_b/R_b$ where σ and μ are the surface tension and dynamic viscosity of liquid, respectively. The pressure of the deriving sound field P_S may be represented by a sinusoidal function such as $P_S = -P_A \sin \omega t$ where P_A is the deriving sound amplitude $\omega = 2\pi f$ and f is frequency. The mass and momentum equations in spherical symmetry given as follows should be solved to understand the gas behavior inside a bubble.

$$\frac{\partial \rho_g}{\partial t} + \frac{1}{r^2}\frac{\partial}{\partial r}(\rho_g u_g r^2) = 0, \quad (2)$$

$$\frac{\partial}{\partial t}(\rho_g u_g) + \frac{1}{r^2}\frac{\partial}{\partial r}(\rho_g u_g^2 r^2) + \frac{\partial P_b}{\partial r} = 0, \quad (3)$$

where r is the distance from center, ρ_g is the gas density, and u_g is the gas velocity which obeys $u_g(R_b, t) = U_b$. The solutions satisfying Eqs. (2) and (3) have been obtained by Kwak and Yang [7]. These are given with time derivative notation as

$$\rho_g = \rho_0 + \rho_r, \quad (4a)$$

$$u_g = \frac{\dot{R}_b}{R_b} r, \quad (4b)$$

$$P_b = P_{b0} - \frac{1}{2}\left(\rho_0 + \frac{1}{2}\rho_r\right)\frac{\ddot{R}_b}{R_b} r^2, \quad (4c)$$

where $\rho_0 R_b^3 = \text{const.}$ and $\rho_r = ar^2/R_b^5$. The constant a is related to the gas mass inside a bubble as $a/m = 5(1 - N_{BC})/4\pi$, with $N_{BC} = (P_{b0}R_b^3/T_{b0})/(P_\infty R_e^3/T_\infty)$ where T_b and T_∞ are gas and ambient temperatures, respectively, R_e is the equilibrium bubble radius, and subscript 0 denotes properties at the bubble center.

Assuming that the internal energy for the gas inside a bubble is a function of gas temperature only as $de = C_{v,b}dT_b$ where $C_{v,b}$ is a constant volume specific heat, the energy equation without a viscous dissipation term is as follows:

$$\rho_g C_{v,b}\frac{DT_b}{Dt} = -\frac{P_b}{r^2}\frac{d}{dr}(r^2 u_g) - \frac{1}{r^2}\frac{d}{dr}(r^2 q_r), \quad (5)$$

where q_r is the radial component of heat flux inside a bubble. Since the solutions given in Eq. (4) also satisfy the kinetic energy equation, only Eq. (5) needs to be solved. With enthalpy representation of the energy equation, one can eliminate $D/Dt(= \partial/\partial t + u_g \partial/\partial r)T_b$ to obtain

$$\frac{DP_b}{Dt} = -\frac{\gamma P_b}{r^2}\frac{d}{dr}(r^2 u_g) - \frac{(\gamma - 1)}{r^2}\frac{d}{dr}(r^2 q_r). \quad (6)$$

Light emission which occurs just prior to the bubble collapse [3] may be related to the significant increase in bubble wall acceleration during this period. Taking into account the bubble wall acceleration, one may obtain the following equation representing the heat flow rate inside a bubble from Eqs. (4a), (4b), (4c), and (6):

$$\frac{(\gamma - 1)}{r^2}\frac{d}{dr}(r^2 q_r) = -\left[\frac{dP_{b0}}{dt} + 3\gamma P_{b0}\frac{\dot{R}_b}{R_b}\right] + \frac{1}{2}\left(\rho_0 + \frac{1}{2}\rho_r\right) \times \left[(3\gamma - 2)\frac{\dot{R}_b \ddot{R}_b}{R_b^2} + \frac{\dddot{R}_b}{R_b}\right] r^2. \quad (7)$$

 0031-9007/96/77(21)/4454(4)$10.00

Since the temperature rise due to the bubble wall acceleration is a transient phenomenon which occurred during a few nanoseconds, the above equation may be decomposed into

$$\frac{(\gamma - 1)}{r^2}\frac{d}{dr}(r^2 q_0) = -\left[\frac{dP_{b0}}{dt} + 3\gamma P_{b0}\frac{\dot{R}_b}{R_b}\right], \quad (8a)$$

$$\frac{(\gamma - 1)}{r^2}\frac{d}{dr}[r^2(q_r - q_0)] = \frac{1}{2}\left(\rho_0 + \frac{1}{2}\rho_r\right) \times \left[(3\gamma - 2)\frac{\dot{R}_b\ddot{R}_b}{R_b^2} + \frac{\dddot{R}_b}{R_b}\right]r^2. \quad (8b)$$

The solution of Eq. (8a), which is essentially the solution with uniform pressure, is known and is quite good for the behavior of a nonsonoluminescencing bubble [7]. Assuming that the conductivity for gas inside a bubble is $k_g = AT + B$, one can obtain the temperature distribution due to q_0. That is

$$T_b(r) = \frac{B}{A} \times \left[-1 + \sqrt{\left(1 + \frac{A}{B}T_{b0}\right)^2 - 2\eta\frac{A}{B}(T_{bl} - T_\infty)\left(\frac{r}{R_b}\right)^2}\right], \quad (9)$$

where $\eta = (R_b/\delta)/k_l/B$ and k_l is the thermal conductivity of liquid. The thickness of thermal boundary layer δ for thermal conduction may be determined from the mass, momentum, and energy equations for liquid with assumption of the quadratic temperature profile in that zone [7].

Abrupt temperature rise and subsequent quenching due to the bubble wall acceleration and the increase and decrease in the acceleration may be treated in another time scale [8], different from the bubble motion. A solution of Eq. (8b) with no temperature gradient at the bubble center is given by

$$T_b'(r) = -\frac{1}{40(\gamma - 1)k_g}\left(\rho_0 + \frac{5}{21}\rho_r\right) \times \left[(3\gamma - 2)\frac{\dot{R}_b\ddot{R}_b}{R_b^2} + \frac{\dddot{R}_b}{R_b}\right]r^4 + C. \quad (10)$$

The coefficient C may be determined from a boundary condition $k_g dT_b/dr = k_l dT_l/dr$ at the wall where T_l is the temperature distribution in the thermal boundary layer with different thickness δ'. That is

$$C = \frac{1}{20(\gamma - 1)}[(3\gamma - 2)\dot{R}_b\ddot{R}_b R_b + \dddot{R}_b R_b^2] \times \left[\frac{\delta'}{k_l}\left(\rho_0 + \frac{5}{14}\rho_{r=R_b}\right) + \frac{R_b}{2k_g}\left(\rho_0 + \frac{5}{21}\rho_{r=R_b}\right)\right]. \quad (11)$$

The above solution is a formal one in the sense that heat flow rate characterized by the boundary layer thickness δ' and the conductivity of liquid k_l is primarily determined by the radiation heat loss in this situation. The temperature distribution inside a bubble may be estimated from Eqs. (9) and (10) with appropriate values of δ' and k_g. The temperature distribution from Eq. (9) can be regarded as a background one. The gas conductivity at ultrahigh temperatures may be obtained from collision integrals [9]. The boundary layer thickness δ' may be determined from a relation $2\pi k_l R_b^2(T_{bl} - T_\infty)/\delta' = P$ where P is power loss due to bremsstrahlung. However, the value of δ' has been chosen so that proper bouncing motion results after the collapse, which is about 0.1 μm. Without heat loss, that is $\delta' \to \infty$ or $k_g \to 0$, the temperature of the gas inside a bubble goes to infinity as confirmed in numerical calculations [10,11]. For example, one may obtain the maximum temperature up to 10^7 K if one uses $k_g = 0.01$ W/mK.

Figure 1 shows the calculated radius-time curve for the bubble with an equilibrium radius of 4.5 μm driven by the field with a frequency of 26.5 kHz and an amplitude of 1.30 atm. The maximum bubble radius calculated is 22.3 μm while the minimum radius is 0.63 μm with substantial reduction of bouncing motion after the first bubble collapse due to quenching of the gas. The temperature at the collapse point is about 500 K, which is a quite different result compared to the nonsonoluminescing case where temperature maximum is achieved at the collapse point. The density, pressure, and temperature profiles inside a bubble at 400 ps before the collapse are shown in Fig. 2. The distributions obtained suggest that the shock formation inside a bubble hardly occurs during this stage because shock cannot propagate to the region of higher density and pressure. Time dependent bubble wall acceleration and the gas temperature at bubble center are shown in Fig. 3. As can be seen in this figure, a sudden increase and subsequent decrease in acceleration of the bubble wall result in rapid quenching of gas followed by the substantial temperature rise up to 25 000 K, which

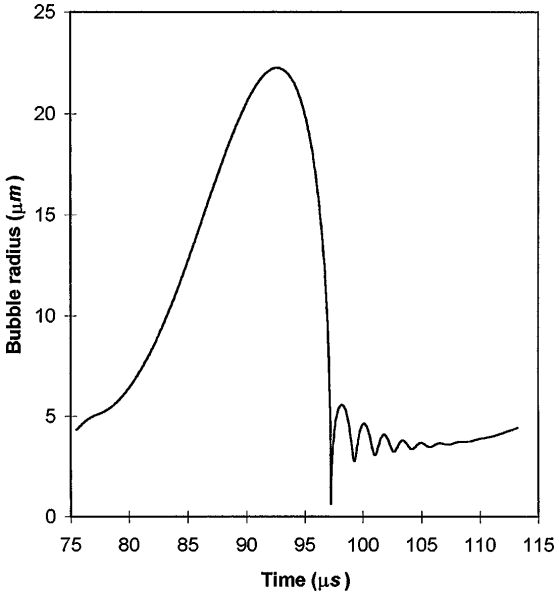

FIG. 1. Theoretical radius-time curve for air bubble of $R_0 = 4.5$ μm at $P_A = 1.30$ atm and $f = 26.5$ kHz in water. Collapse occurs at $t = 97.2134$ μs.

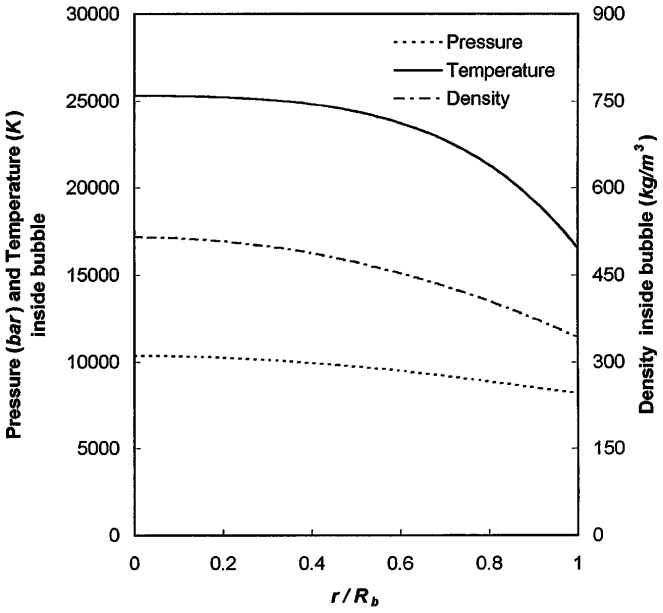

FIG. 2. Density, pressure, and temperature distributions inside a bubble at 400 ps prior to the collapse point for the case shown in Fig. 1.

can be regarded as a thermal spike. Considerable increase in gas temperature due to bubble wall acceleration can be seen in Fig. 3. With uniform pressure approximation [7], the maximum temperature achieved is only 5800 K at the collapse. These calculation results also show why the light emission occurs just prior to the collapse [3] and the duration of the pulse is in the range of 300 ps, which is half the width of the thermal spike. More temperature rise near the bubble collapse can be obtained when the acoustic amplitude increases. For the case of an equilibrium

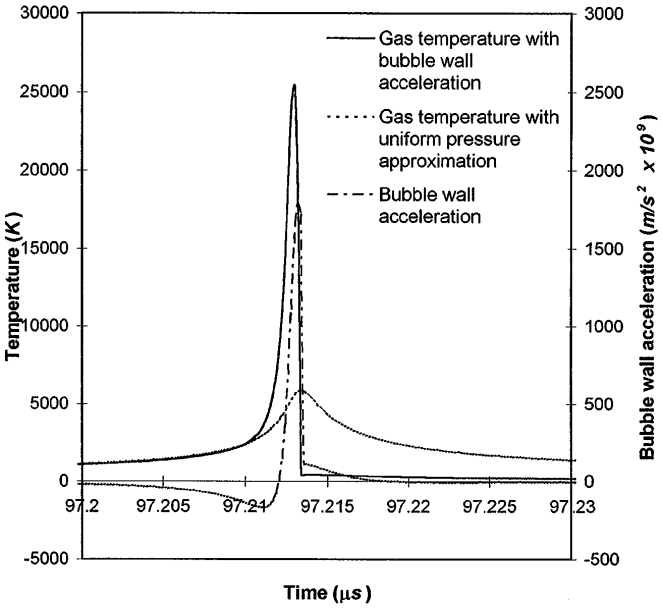

FIG. 3. Time dependent bubble wall acceleration and gas temperature around the collapse point for the case shown in Fig. 1. The maximum occurs at 400 ps prior to the collapse.

radius of 4.0 μm driven by the field with a frequency of 26.5 kHz and an amplitude of 1.40 atm, the maximum center temperature achieved at 400 ps before the collapse is about 100 000 K.

In Table I the sensitivity of sonoluminescence to external parameters is shown. Calculation results show that such extreme sensitivity of SL to external parameters originates from the sudden increase in bubble wall acceleration near the bubble collapse. If the radiation is of thermal blackbody origin, the duration of SL should be greater than 100 ns, as can be seen in Fig. 3. Moreover, black body radiation is an equilibrium phenomenon, and it may not explain such a transient occurrence.

Even though thermal black body radiation shows continuous spectrum, observed results from SL cannot be explained by thermal radiation as mentioned before. The other possibility of continuous spectrum is bremsstrahlung due to electron-ion collision. The emission coefficient j_ω due to bremsstrahlung from the gas volume is given by [12]:

$$j_\omega = n_i n_e Z^2 V_B \left(\frac{e^2}{4\pi\varepsilon_0}\right)^3 \left(\frac{m_e}{2\pi k T_e}\right)^{1/2} \frac{1}{m_e^2 c^3} \frac{4}{3\pi} \times \left[\frac{\pi}{\sqrt{3}}\,\overline{G}(T,\omega)\right], \tag{12}$$

where n_i and n_e are the densities of ions and electrons in bubble volume V_B, respectively, ε_0 is the dielectric constant for free space, and c is the speed of light. The electron temperature T_e is obtained by assuming a Maxwellian electron velocity distribution. At a high frequency regime (Born approximation), the Gaunt factor obtained by summation over the electron velocity distribution [12] is $\overline{G}(T,\omega) = \sqrt{3/\pi}\,\exp(-\hbar\omega/kT_e)/\sqrt{\hbar\omega/kT_e}$. The corresponding spectral radiance turns out to be $j_\lambda = \omega^2 j_\omega/(2\pi c)$, which is proportional to $\omega^2 \exp(-\hbar\omega/kT_e)/\sqrt{\hbar\omega/kT_e}$ or $\exp(-hc/kT_e\lambda)/\sqrt{hc/kT_e\lambda}/\lambda^2$, where λ is wavelength. Thus one can see that the emission intensity falloff is $\exp(-\hbar\omega/kT_e)$ at frequencies of $\hbar\omega/kT_e \geq 1$. Consequently, the spectral radiance is maximum when $dj_\lambda/d\omega = 0$, which results in $\lambda_{\max} = 2hc/(3kT_e)$, and the emission intensity varies as $1/\lambda^{2.5}$ as observed in experiments. The total emission of bremsstrahlung is obtained by integrating j_ω over all frequencies. The result is found to be for one polarization, which is given by

$$j = n_i n_e Z^2 V_B \left[\frac{4\pi^3}{3}\left(\frac{8kT_e}{\pi m_e}\right)^{1/2}\left(\frac{e^2}{4\pi\varepsilon_0}\right)^3\left(\frac{1}{m_e c^3 h}\right)\right] \times \frac{4}{\sqrt{3}\,\pi}\,\overline{G}/8\pi\,. \tag{13}$$

The calculated SL spectrum depending wavelength from a bubble of 2% Xe in N_2 with an equilibrium radius of 4.5 μm driven by the field with a frequency of 26.5 kHz and an amplitude of 1.32 atm is shown in Fig. 4. The peak temperature in this case is about 32 000 K. Even though the intensity is quite a bit larger than the observed

TABLE I. Calculated gas temperature at bubble center and the maximum bubble wall acceleration depending on the equilibrium bubble radius, the driving amplitude of ultrasound, and ambient liquid temperature.

		Case 1	Case 2	Case 3	Case 4 (No SL)
Experimental	R_0 (μm)	5.5	4.5	4.0	8.5
input	P_A (atm)	1.25	1.3	1.4	1.075
parameter	T_∞ (K)	308	293	276	293
Calculation	$\ddot{R}_b$ (m/s^2)	1.02×10^{12}	1.79×10^{12}	4.82×10^{12}	2.38×10^{10}
results	T_c (K)	13 000	25 000	100 000	2400

data [4], the qualitative trend is similar to experimental results. A spectral peak occurs at 300 nm, which implies that the average electron velocity is about 3×10^6 m/s. If the electron velocity or temperature increases, the peak is shifted to shorter wavelength. In this case the total emission is about 4 mW/sr, which is in close agreement with the observed value [2], considering measurement angle (sr). If the gas temperature increases to 100 000 K, the emissive power is about 150 mW/sr. Note that the contribution from nitrogen ions is not considered because the relaxation time for the dissociation of N_2 [13] is greater than the excursion time of the thermal spike so that the dissociation of N_2 hardly occurs during this time.

The emissive power, as can be seen from Eq. (13), depends on the density of electrons and ions, the species of ion, and the kinetic energy of the electron. The numerical value of a typical density of ions near collapse is about $5 \times 10^{25}/\mathrm{m}^3$. These parameters shaping the spectrum of SL are determined by the maximum values of gas temperature and pressure achieved during the collapse. The power spectrum given in Eq. (13) is the case for an isotropic distribution of electrons. If the electron distribution is an anisotropic one, different spectrum may be obtained [14]. Detailed analysis and discussions are presented in another paper [15].

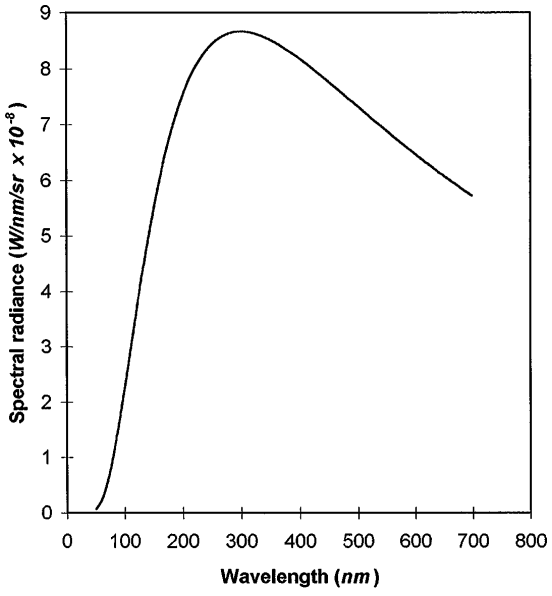

FIG. 4. Spectral radiance (W/μm/sr) from the 2% Xe bubble in nitrogen. Initial bubble radius is $R_0 = 4.5$ μm with an ultrasound amplitude of $P_A = 1.32$ atm at $f = 26.5$ kHz.

This work has been supported in part by grants from the Korea Science and Engineering Foundation under Contract No. 95-0200-03 and from Chung-Ang University.

[1] D. F. Gaitan, L. A. Crum, C. C. Church, and R. A. Roy, J. Acoust. Soc. Am. **91**, 3166 (1992).
[2] R. Hiller, S. J. Putterman, and B. P. Barber, Phys. Rev. Lett. **69**, 1182 (1992).
[3] B. P. Barber and S. J. Putterman, Phys. Rev. Lett. **69**, 3839 (1992).
[4] R. Hiller, K. Weninger, S. J. Putterman, and B. P. Barber, Science **266**, 248 (1994).
[5] L. A. Crum and R. A. Roy, Science **266**, 233 (1994).
[6] J. B. Keller and M. Miksis, J. Acoust. Soc. Am. **68**, 628 (1980).
[7] H. Kwak and H. Yang, J. Phys. Soc. Jpn. **64**, 1980 (1995).
[8] R. C. Davidson, *Methods in Nonlinear Plasma Theory* (Academic Press, New York, 1972).
[9] M. I. Bonlos, P. Fanchais, and E. Pfender, *Thermal Plasmas* (Plenum, New York, 1994), Vol. 1.
[10] C. C. Wu and P. H. Roberts, Phys. Rev. Lett. **70**, 3424 (1993).
[11] W. C. Moss, D. B. Clarke, J. W. White, and D. A. Young, Phys. Fluids **6**, 2979 (1994).
[12] G. Bekefi, *Radiation Processes in Plasmas* (John Wiley and Sons, New York, 1966).
[13] Ya. B. Zeldovich and Yu. P. Raizer, *Physics of Shock Waves and High Temperature Hydrodynamic Phenomena* (Academic Press, New York, 1966), Vol. 1.
[14] T. Chou and E. G. Blackman, Phys. Rev. Lett. **76**, 1549 (1996).
[15] H. Kwak and J. Na (to be published).